A Self-Compensated Planar Coil for Resonant Wireless Power Transfer Systems

Qingsong Wang, *Member, IEEE*, Mohammad Ali Saket, *Student Member, IEEE*, Aaron Troy, and Martin Ordonez, *Member, IEEE*,

***Abstract*— Compensation capacitors are important components of any resonant wireless power transfer (RWPT) systems and significantly affect the output power, operating frequency, and efficiency. Depending on the compensation network, these capacitors can be placed in series or parallel with the coils. The physical capacitor reduces reliability and increases the size and cost of RWPT systems. Self-resonant RWPT systems have been proposed to remove physical capacitor, but have to work with high frequency, several megahertz, as reported in existing literatures. In this paper, a new planar coil that utilizes parallel-connected multi-layer Printed Circuit Boards (PCB) to generate large parasitic capacitance, is proposed for RWPT. Both transmitter and receiver coils are made using PCB coils and a spiral winding layout is used to achieve the required inductance and capacitance. Benefit from large parasitic capacitance, the resonant frequency of the proposed RWPT system is reduced to below 200 kHz. Meanwhile, because of the elimination of physical capacitance, the proposed RWPT system has a compact structure, improved reliability, and reduced size, weight, and cost. A coil prototype is designed, constructed and tested. Simulation and experimental investigations validate the effectiveness of the proposed design.**

***Index Terms* - Intra-winding capacitance, Planar coil, Resonant wireless power transfer (RWPT), Self compensation**

I. Introduction

Wireless power transfer (WPT) systems are attracting increased attention in various applications, such as electric vehicles (EVs) [1], portable electronics [2], implantable medical devices [3], and underwater equipment [4]. The essential principle of WPT is based on electromagnetic induction: when an alternating power is applied to the transmitter, voltage is induced on the receiver, which can output electric power to the load. Early WPT systems were very similar to transformers, with a gap between the primary and secondary coils [5]. In order to transfer power with high efficiency, strong coupling between the transmitter and receiver is desired, but this limits the application of WPT systems to short-distance power transfer. Meanwhile, accurate alignment between the transmitter and receiver is also needed to ensure strong coupling.

A new era of WPT began when researchers from MIT first proposed resonant WPT (RWPT) in 2007 [6], with the achievement of fully lightening a 60 W light bulb over a distance of 2 m. Both the transmitter and receiver are separately connected with a capacitor to form a resonant tank, and high-efficiency power transfer can be achieved even when the transmitter and receiver are loosely coupled, which significantly increases the power transfer distance. One major component of RWPT systems is the magnetic coil, the design of which has a significant influence on the power, efficiency, and misalignment tolerance. Circular coils are the most common architecture due to their simple structure and single-sided flux, which ensures minimal losses and low leakage [7]. Because of the unipolar flux, circular coils have limited power transfer distance and poor tolerance to horizontal misalignment. An improved structure, called DD coil, is proposed in [8]. Bipolar flux is achieved and the flux path height of DD coil can be twice as large as the circular coil, significantly increasing the power transfer distance. Further improvement on the tolerance to horizontal misalignment can be achieved by adding a quadrature coil to the receiver [9]. In [10], a unipolar coil and bipolar coil are integrated to form a compact magnetic coupler while delivering high power. The coils at the same side are naturally decoupled, and a peak efficiency of 94% is reported. Introducing additional resonators is a good way to ensure high efficiency, which results in three-coil RWPT [11]–[14] and four-coil RWPT [15]–[17] systems. The intermediate coils are designed for impedance matching, which enables high-efficiency operation even under a week coupling, and extends the transmission distance. In order to achieve better tolerance to misalignment, omnidirectional coils [18], [19] have been investigated, which allow more lateral and angular misalignments, because the magnetic flux can flow in all directions and the receiver can pick up energy in any position. The structure of omnidirectional coils is more complicated and restricts their wide application.

The compensation network, which usually consists of a capacitor placed in series or parallel with the coil to form a resonant tank. The function of the compensation capacitor is to minimize the volt-ampere (VA) rating of the power supply at the transmitter side and to maximize the power transfer capability of the receiver. Generally, there are four basic types of compensation topologies: series-series (SS), series-parallel (SP), parallel-series (PS), and parallel-parallel (PP) [20]–[23]. SS compensation is the most commonly used one, because the resonant frequency is independent of the load and coupling coefficient. However, a large bridge capacitor is needed at

Manuscript received November 10, 2019; revised February 11, 2020 and April 10, 2020; accepted May 14, 2020. This work was supported by the Natural Sciences and Engineering Research Council (NSERC), Canada.

Qingsong Wang is with the Centre for Advanced Low Carbon Propulsion Systems (C-ALPS), Coventry University, Coventry CV1 5FB, United Kingdom (e-mail: qingsongwang@ieee.org).

Mohammad Ali Saket, Aaron Troy and Martin Ordonez are with the Department of Electrical and Computer Engineering, The University of British Columbia, Vancouver, BC V6T 1Z4, Canada (e-mail: mohammadali.saket@gmail.com; amichaeltroy@gmail.com; mordonez@ieee.org).

This article has been accepted for publication in a future issue of this journal, but has not been fully edited. Content may change prior to final publication. Citation information: DOI 10.1109/TPEL.2020.2998186, IEEE Transactions on Power Electronics

the output of the rectifier in order to achieve continuous conduction, which increases the control difficulty of the start-up stage [24]. Another drawback of SS topology is that there are large voltages across the power pad, which lead to large currents and limit SS compensation to low-power applications. SS compensation is also very sensitive to misalignment, because the power is inversely proportional to the square of the coupling coefficient [25]. PP compensation has better tolerance of misalignment, but has low power factor and low efficiency because of the imaginary impedance. When PP compensation is connected with a voltage source, large current spikes appear at the switching transitions as the capacitor is charged or discharged by the inverter. To incorporate the advantages of both the SS and PP compensation topologies, inductor-capacitor-inductor (LCL) topologies have been investigated [25]–[27]. The imaginary impedance can be canceled by an additional inductor, allowing the power factor to be improved. LCL compensation is very suitable for high-power applications because the inverter current is very small compared to pad currents. Compared with SS compensation, LCL is less sensitive to misalignment. Current spikes in PP compensation are also eliminated, by including an additional inductor. All the aforementioned compensation networks use additional passive elements, a capacitor or a combination of capacitor and inductor. A self-resonant RWPT is proposed in [28], in which the parasitic capacitance between the top layer and bottom layer of a printed circuit board (PCB) coil is used for compensation, in series with the coil inductance. However, only a very small capacitance is obtained through the design, and the proposed WPT system has to work at a high frequency, 6.78 MHz as reported.

In this paper, a new self-compensated planar coil is proposed for RWPT systems. Intra-winding capacitance is used to replace the physical compensation capacitor, and accordingly reduce the size and cost, and improve reliability as well. Through connecting several multi-layer PCB coils in parallel, large parasitic capacitance can be obtained, which brings the self-resonant frequency below 200 kHz. In order to cancel imaginary impedance, an additional inductor is connected to both the transmitter and receiver to form an LCL resonant tank, which enables the RWPT system to operate with a high power factor. This paper is organized as follows: the coil structure and the analysis of the circuit are presented in Section II; performance evaluation through simulation is given in Section III, experimental validation is conducted in Section IV; and finally the conclusion is summarized in SectionV.

II. Coil Structure and Circuit Analysis

A. Double-layer PCB Coil

The idea presented in this paper is to use the intra-winding capacitance for compensation in order to achieve the self-resonance. A double-layer PCB with a spiral coil winding layout is shown in Fig. 1 (a). Both transmitter and receiver consist of two spiral coils on the top and bottom layers of a double-layer PCB, which are connected in series through a center point. The PCB material (which is between the top and bottom layers) is FR4 and the parasitic capacitance that is formed between the top and bottom layers is referred to as intra-winding capacitance. The intra-winding capacitance and coil inductance, which are in parallel, form a resonant tank. The calculation of intra-winding capacitance has been reported in [29]. When applied with a voltage V, the total

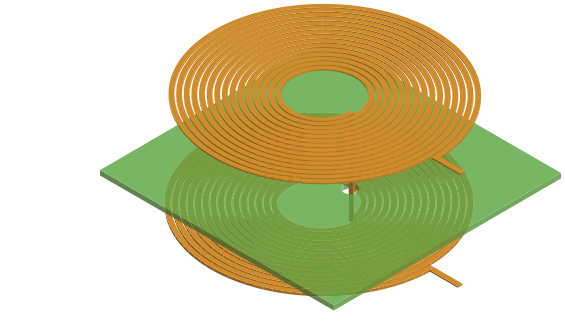

(a)

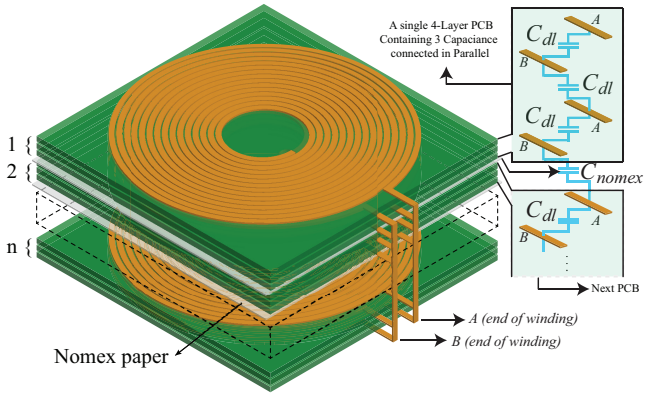

(b)

Fig. 1: Structure of the proposed self-compensated planar coil. a) Double-layer PCB coil and, b) Parallel connected multi-layer PCB coils.

energy stored in the coil can be expressed as

$$W_t = \int_0^L \frac{1}{2}\frac{\epsilon_0\epsilon_r W}{d}(V - \frac{V}{2L}x - \frac{V}{2L}x)^2 dx = \frac{1}{2}\frac{\epsilon_0\epsilon_r WL}{3d}V^2 \quad (1)$$

In (1), ϵ_0 and ϵ_r are the vacuum permittivity and relative permittivity of dielectric material FR4, respectively. W is the trace width and L is the total length of a single-layer spiral coil. The lumped equivalent capacitance is then given by one-third of the static capacitance:

$$C_{dl} = \frac{\epsilon_0\epsilon_r WL}{3d} \quad (2)$$

It is clear that the intra-winding capacitance is proportional to the interleaving area of the top and bottom layers. Therefore, the coil should have a large diameter to get enough capacitance, which increases the size and resistance.

B. Multi-layer PCB Coils in Parallel

In order to increase intra-winding capacitance, an improved design is shown in Fig. 1 (b). Multi-layer PCB coils connected in parallel are employed, and Nomex paper is placed between adjacent PCB coils for insulation. In this case, every two adjacent coil layers have an intra-winding capacitance, and all these capacitances are

This article has been accepted for publication in a future issue of this journal, but has not been fully edited. Content may change prior to final publication. Citation information: DOI 10.1109/TPEL.2020.2998186, IEEE Transactions on Power Electronics

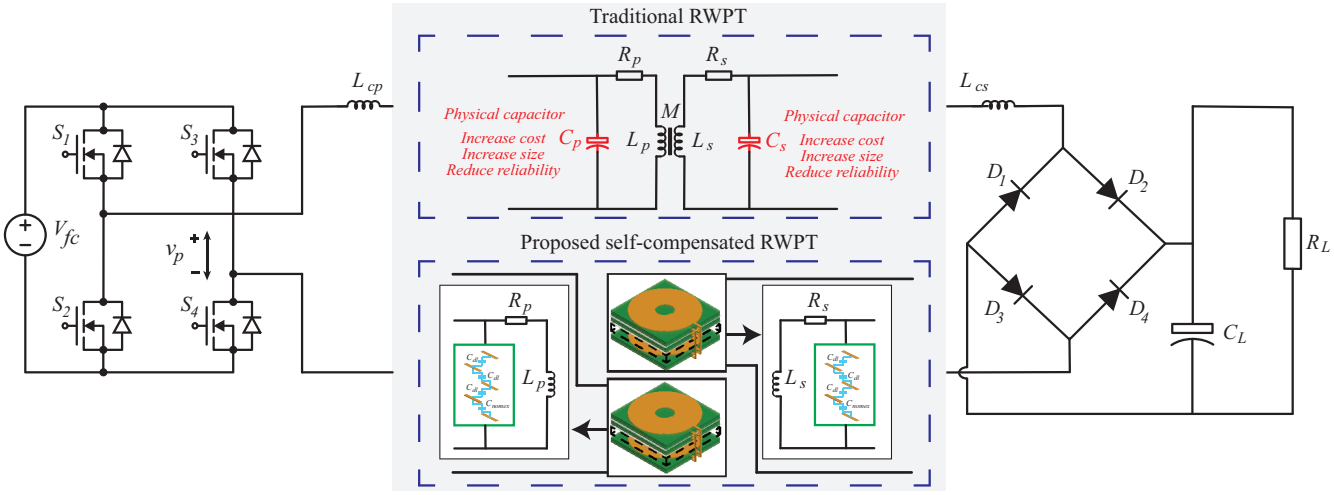

Fig. 2: Schematic circuit diagram of traditional RWPT and the proposed self-compensated RWPT system.

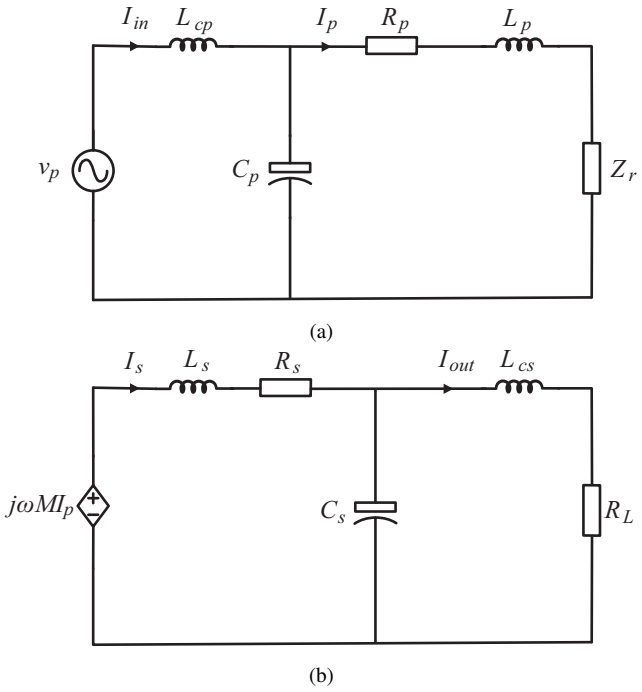

Fig. 3: Equivalent circuits of (a) the transmission network, and (b) the receiver network.

in parallel. The total capacitance is the sum of individual intra-winding capacitances, and can be calculated using the following equation:

$$C_0 = n(k-1)C_{dl} + (n-1)C_{nomex} \tag{3}$$

In (3), C_{nomex} is the capacitance generated by the coils adjacent to the Nomex paper and k and n are the numbers of PCB layers and PCB coils, respectively. From this equation, we can see that the intra-winding capacitance is directly proportional to the number of layers in a PCB and also to the number of PCBs connected in parallel. It can therefore be increased by increasing the number of PCB layers and coils. Meanwhile, resistance is reduced because of the parallel connection of the coils. Therefore, the proposed RWPT system can operate at a low resonant frequency.

C. Circuit Analysis

The schematic circuit diagram of this coil is shown in Fig. 2. A full-bridge inverter is used to generate v_p, while a full bridge rectifier is used to apply a DC voltage to R_L. C_p, R_p, L_p and C_s, R_s, L_s are the intra-winding capacitance, AC resistance and self-inductance of the transmitter and receiver, respectively. M is the mutual inductance between transmitter and receiver. The shadow in Fig. 2 indicates that intra-winding capacitance is used for compensation and no additional physical capacitor is used, which means this coil integrates inductance and compensation capacitance in the same structure, and can achieve self-compensation. Because the intra-winding capacitance is in parallel with the inductance, the reflected impedance from the load to the transmitter side has an imaginary part that varies with the changes in load resistance. In order to achieve high power factor operation, impedance matching inductors L_{cp} and L_{cs} are employed in series with the transmitter and receiver, respectively. Therefore, LCL compensation is performed and the proposed WPT system can operate with a high power factor.

For simplicity, the transmitter and receiver in this paper have the same design parameters and the turn ratio is 1:1. That is:

$$\begin{aligned} R_p &= R_s = R_0 \\ L_p &= L_s = L_0 \\ C_p &= C_s = C_0 \end{aligned} \tag{4}$$

In order to achieve a unique resonant frequency for both the transmitter and receiver, the impedance matching inductance should have the same value as the self-inductance of the transmitter and receiver. The equivalent circuits of the transmitter and receiver are shown in Fig. 3.

$$\begin{aligned} L_{cp} &= L_p = L_0 \\ L_{cs} &= L_s = L_0 \end{aligned} \tag{5}$$

This article has been accepted for publication in a future issue of this journal, but has not been fully edited. Content may change prior to final publication. Citation information: DOI 10.1109/TPEL.2020.2998186, IEEE Transactions on Power Electronics

And the resonant frequency can be expressed as

$$\omega_0 = \frac{1}{\sqrt{C_0 L_0}} \tag{6}$$

The transmitter circuit acts as a voltage source in the receiver side circuit. An equivalent resistance R_L is used, as the load and rectifier are not considered in the receiver circuit. The impedance of the receiver circuit can be expressed as

$$Z_s = j\omega L_s + R_s + \frac{1}{j\omega C_s} \| (j\omega L_{cs} + R_L) \tag{7}$$

When the proposed RWPT works at the resonant frequency, Z_s can be rewritten as

$$Z_s = R_0 + \frac{L_0}{C_0 R_L} \tag{8}$$

It can be observed that Z_s only has a real component at the resonant frequency. The impedance of receiver side circuit can be reflected to the transmitter circuit, which is Z_r as shown in Fig. 3(b).

$$Z_r = \frac{\omega_0^2 M^2}{Z_s} \tag{9}$$

It is clear that Z_r is also resistive at the resonant frequency. The total impedance seen from the input voltage source, Z_{in}, can be expressed as

$$Z_{in} = j\omega L_{cp} + \frac{1}{j\omega C_p} \| (j\omega L_p + R_p + Z_r) \tag{10}$$

At resonant frequency, Z_{in} can be simplified as shown in (11)

$$Z_{in} = \frac{L_0}{(R_0 + Z_r) C_0} \tag{11}$$

Again, the input impedance has no imaginary part, so theoretically the proposed RWPT system can achieve unique power factor (UPF) operation. The circuit equations can be expressed as

$$\begin{aligned} U_{in} &= I_{in} Z_{in} \\ U_{in} &= I_{in} j\omega L_0 + I_p (j\omega L_0 + R_0 + Z_r) \\ j\omega M I_p &= I_s Z_s \\ j\omega M I_p &= I_s (j\omega L_0 + R_0) + I_{out} (j\omega L_0 + R_L) \end{aligned} \tag{12}$$

The resonant currents are given by solving the equations:

$$\begin{aligned} I_{in} &= \frac{U_{in}}{Z_{in}} \\ I_p &= \frac{U_{in}\{(1-\omega_0^2 L_0) R_0 - j\omega_0 [L_0 + (R_0 + Z_r)(R_0 + C_0 Z_r)]\}}{\omega_0^2 L_0^2 + (R_0 + Z_r)^2} \\ I_s &= \frac{j\omega_0 M I_p}{Z_s} \\ I_{out} &= \frac{\omega_0 M I_p \{\omega_0 L_0 (1 + R_L - R_0) + j[R_L (1 - R_0) - \omega_0^2 L_0^2]\}}{Z_s (\omega_0^2 L_0^2 + + R_L^2)} \end{aligned} \tag{13}$$

The output power and coil to coil efficiency can be expressed as

$$\begin{aligned} P_{out} &= I_{out}^2 R_L \\ \eta &= \eta_t \eta_r = \frac{Z_r}{Z_r + R_0} \frac{Z_s - R_0}{Z_s} \end{aligned} \tag{14}$$

III. Performance Evaluation

In this section, an example PCB coil is designed as the self-compensated transmitter and receiver, and the performance of the RWPT system is investigated through simulation. Figure 4 shows the output power and efficiency when the RWPT system is designed with different resonant frequencies. In this simulation, the inverter and rectifier are eliminated, the RWPT system is directly supplied by an AC voltage source, and a resistor is used as the equivalent load. It can be observed that the resonant frequency has minimal influence on the output power. When the coupling coefficient k increases from 0.3 to 0.5, there is a slight increase in output power. The behavior of efficiency is different and higher resonant frequency will produce a higher efficiency. However, the efficiency shown in Fig. 4(b) is only the coil to coil efficiency; the whole efficiency of RWPT system should also take the inverter and rectifier into consideration. Since higher frequency leads to higher switching loss in the inverter and rectifier, the resonant frequency of the RWPT system cannot be designed to be as high as possible.

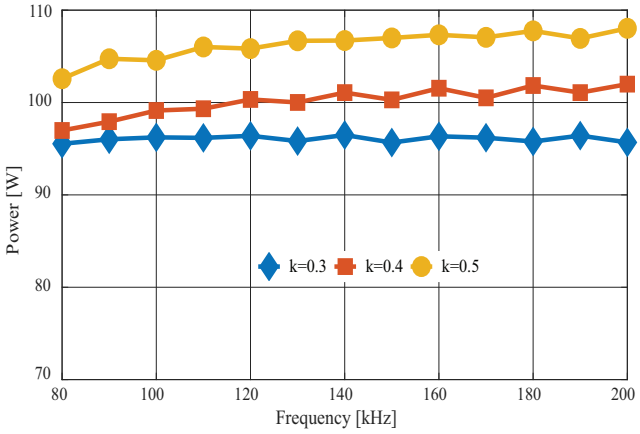

(a)

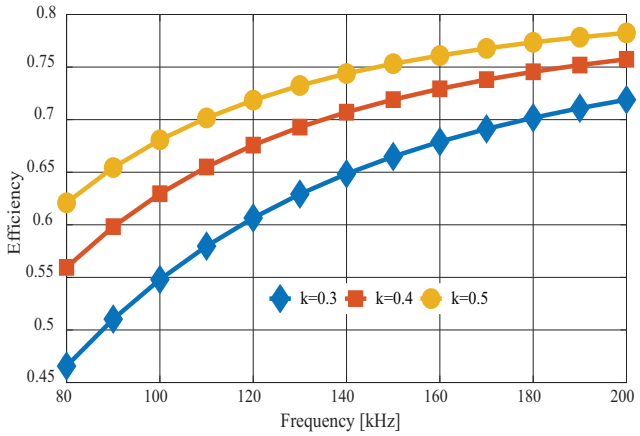

(b)

Fig. 4: Power and efficiency at different resonant frequencies.a) Power curves and, b) Efficiency curves.

The geometrical parameters have a significant influence on both the inductance and the capacitance, especially the inner radius and the number of turns. The coil turns close to the center make a limited contribution to inductance and capacitance due to their small radius, but they have a large AC resistance because of strong magnetic flux density. Therefore, it is a good idea to remove

This article has been accepted for publication in a future issue of this journal, but has not been fully edited. Content may change prior to final publication. Citation information: DOI 10.1109/TPEL.2020.2998186, IEEE Transactions on Power Electronics

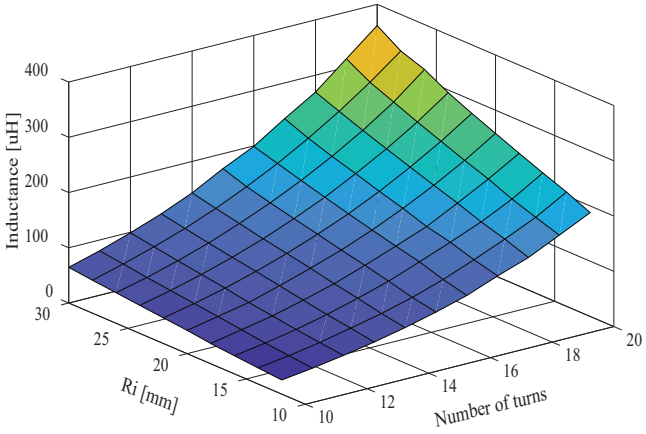

(a)

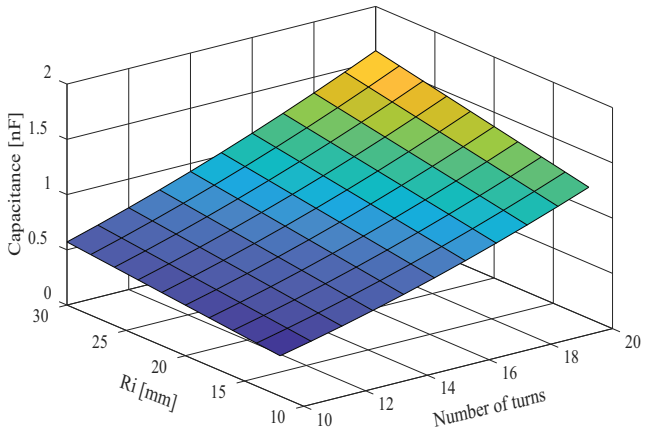

(b)

Fig. 5: Influence of inner radius and turn number on coil inductance and intra-winding capacitance. a) Inductance and, b) Intra-winding capacitance.

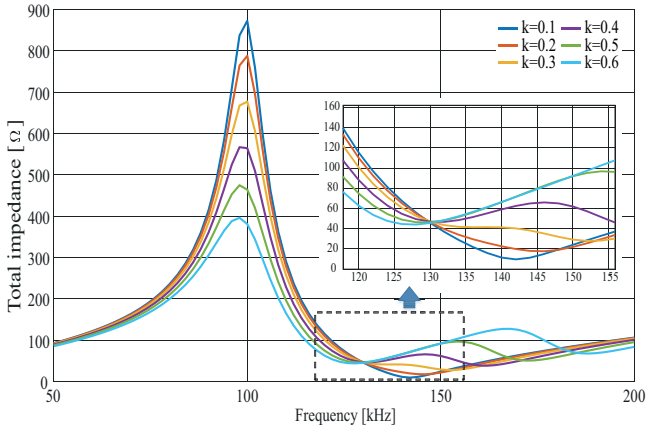

(a)

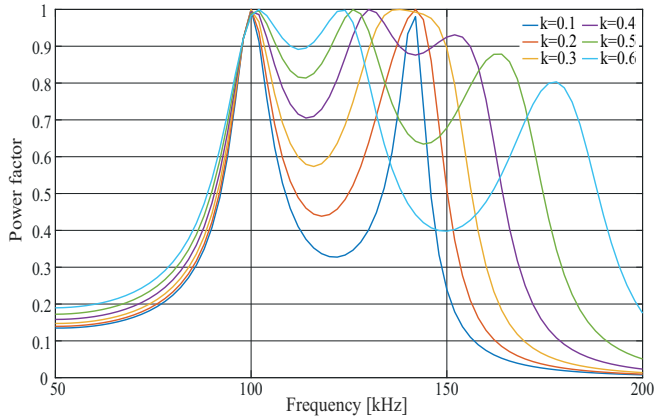

(b)

Fig. 6: Total impedance and power factor at different frequencies. a) Total impedance and, b) Power factor.

part of the coil turns to create a hollow winding. The inductance is proportional to the square of the number of turns, and the capacitance is also positively related to the number of turns if the trace width is fixed. Fig. 5 shows the influence of the inner radius and the number of turns on the inductance and capacitance of a double-layer PCB coil. This figure shows that both inductance and capacitance increase as the inner radius and number of turns increase. Compared to the number of turns, the influence of the inner radius is less significant. It should be noted that a large inner radius and number of turns also means larger coil size, and therefore a trade-off should be considered during the coil design process.

From Fig. 5(b), it can be observed that only very small intra-winding capacitance can be obtained from a double-layer PCB coil, so a parallel-connected multi-layer PCB is employed to obtain larger capacitance. Although various combinations of PCB layers and coil number can be considered, there exists a lower limit on the dielectric layer thickness. Additionally, a thinner dielectric layer presents a higher overall cost. Commercial low-cost PCBs are usually made in 4-layer structures with the total thickness of

TABLE I: Design Parameters

Item	Value
Inner radius	$22mm$
Trace width	$3.5mm$
Inter-turn gap	$0.5mm$
Number of turns	15
Trace thickness	$0.07mm$
Thickness of dielectric layer	$0.24mm$
Thickness of insulation paper	$0.178mm$
Thickness of ferrite board	$3.8mm$
PCB layers	4
Number of PCB	6
Number of ferrite board	1

$1.6mm$. While PCB manufacturers can do customized PCB for different number of layers and different thicknesses, the cost of such PCBs are significantly higher. In this project, we used low-cost 4-layer PCBs and then adjusted the number of PCBs to achieve

This article has been accepted for publication in a future issue of this journal, but has not been fully edited. Content may change prior to final publication. Citation information: DOI 10.1109/TPEL.2020.2998186, IEEE Transactions on Power Electronics

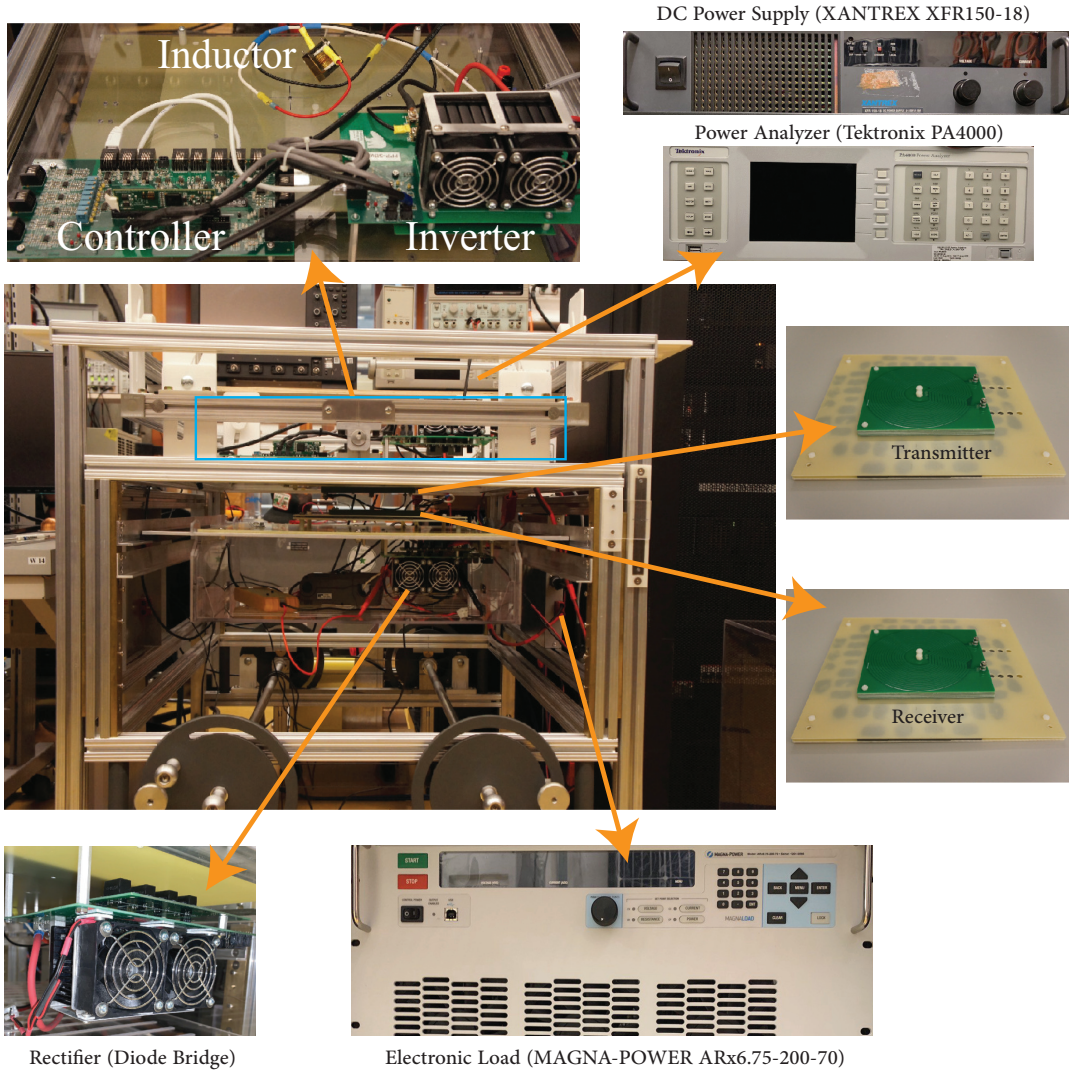

Fig. 7: Experimental platform used to measure the performance of the proposed RWPT system.

the desirable capacitance. The inner radius and number of turns are designed as 22 mm and 15, respectively. A ferrite board is used to enhance the flux of transmitter and receiver. The detailed design parameters of the coil are listed in Table I. One of the important features of the LCL compensated RWPT system is unit power factor (UPF) at the resonant frequency. Figure 6 shows the input impedance and power factor, when the RWPT system operates at different frequencies. It can be observed that there are two UPF frequencies, and the higher UPF frequency reduces with the increasing of coupling coefficient. In order to transmit maximum power, the system should operate with the lowest impedance point, therefore the higher UPF frequency should be selected as the working frequency.

IV. Experimental Verification

In this section, a prototype with the parameters given in Table. I is manufactured, and experimental measurements are conducted to verify the effectiveness of the proposed self-compensated coil. The experimental platform and prototype are shown in Fig. 7. This platform has four degrees of freedom. The transmission distance, horizontal misalignment, and angular misalignment around both x and y-axis can be adjusted through mechanical handles, and the corresponding performance can be investigated. The proposed RWPT system is supplied by a DC power source (XANTREX XFR150-18), and a power analyzer (Tektronix PA4000) is used to measure the input and output power. The load is provided by an electronic load (MAGNA-POWER ARx6.75-200-70). MOSFET IRFP4868PBF is used to build the inverter and diode VS-60APH03-N3 is used to build the rectifier. The measured inductance and capacitance are $129\mu H$ and $20nF$, respectively, which have a good match with simulation results. Fig. 8(a) shows the coupling coefficient at different transmission distances, and Fig. 8(b) shows the coupling coefficient with horizontal misalignment. It can be observed that the measured coupling coefficient is slightly

This article has been accepted for publication in a future issue of this journal, but has not been fully edited. Content may change prior to final publication. Citation information: DOI 10.1109/TPEL.2020.2998186, IEEE Transactions on Power Electronics

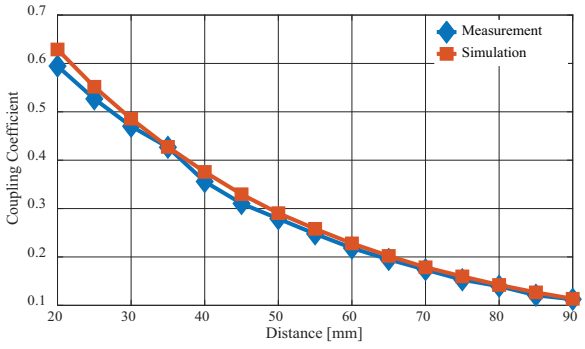

(a)

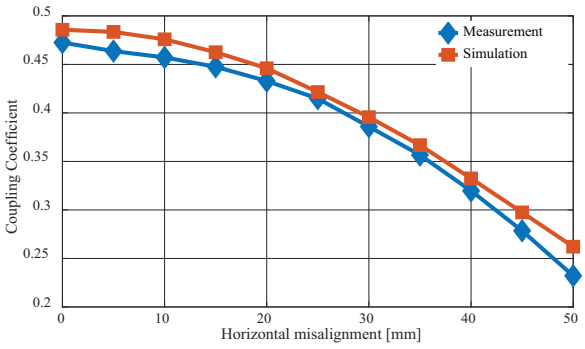

(b)

Fig. 8: Coupling coefficient. a) Coupling coefficient at different transmission distances, no misalignment and, b) Coupling coefficient with horizontal misalignment, when transmission distance is 30mm.

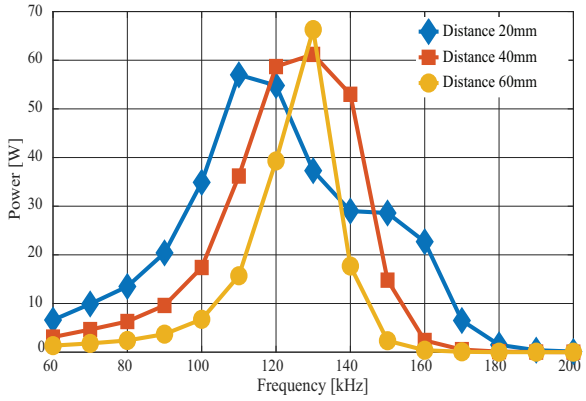

Fig. 9: Output power at different frequencies, when the transmission distances are 20mm, 40mm, and 60mm.

lower than the simulation result. The reason is because simulation does not consider the influence of glue used to assemble the coils. When we made the prototype, all the ferrites were glued on a plastic board and then the PCBs were placed on the other side of the board. The applied glue is very thin, but increases the gap between the winding and ferrite and so results in a slightly lower coupling coefficient than that predicted by the simulation.

Fig. 9 shows the output power at different frequencies, when

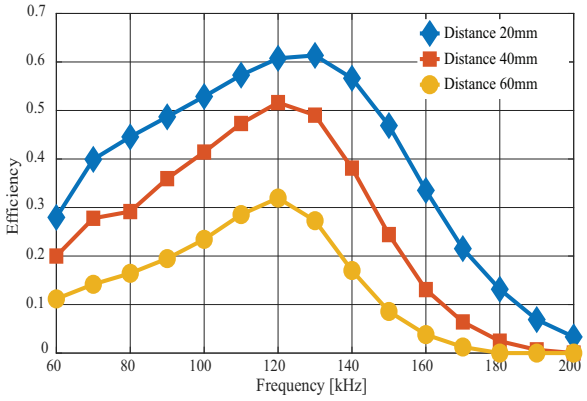

Fig. 10: Efficiencies at different frequencies, when the transmission distances are 20mm, 40mm, and 60mm.

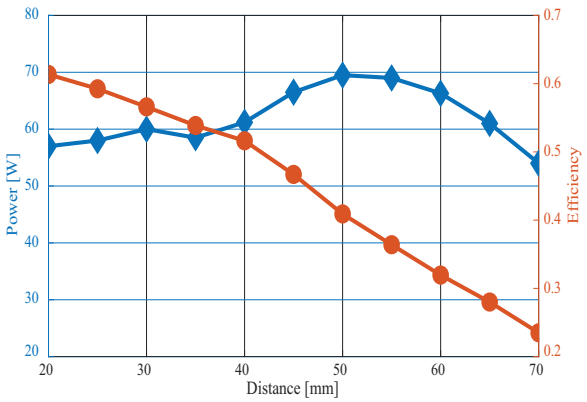

Fig. 11: Output power and efficiencies at different transmission distances, when the load is 70 Ω.

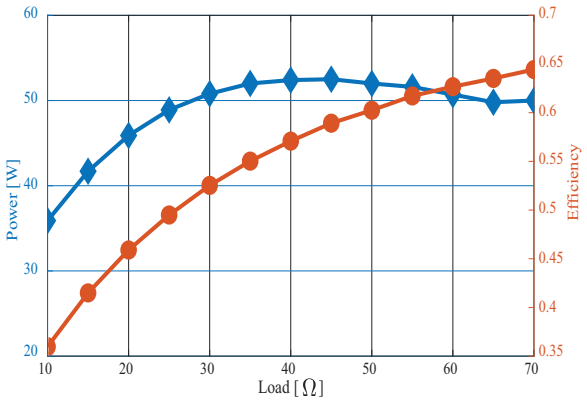

Fig. 12: Output power and efficiencies when the load changes, transmission distance 20mm.

the transmission distances are $20mm$, $40mm$, and $60mm$, respectively. It can be observed that maximum power appears when the frequency is around $120kHz$, which is close to the higher UPF frequency with the lowest impedance, as shown in Fig. 6. The

This article has been accepted for publication in a future issue of this journal, but has not been fully edited. Content may change prior to final publication. Citation information: DOI 10.1109/TPEL.2020.2998186, IEEE Transactions on Power Electronics

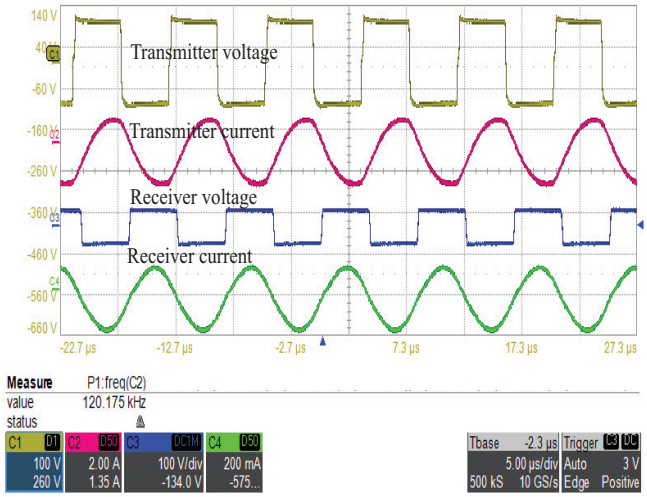

Fig. 13: Steady state voltage and current waveform of transmitter and receiver.

maximum power frequency is not exactly the same as the higher UPF frequency because zero voltage switching (ZVS) is employed during the measurement, and this requires a small phase difference between the input voltage and current, making the maximum power appears at a lower frequency. Currently, we are running the prototype at 67W to show the proof of concept. However, the power can be pushed further if proper means for cooling is used. The efficiency shows similar characteristics, as shown in Fig. 10, the maximum efficiency appears around 120 kHz. When the load is 70Ω, the output power and efficiency at different transmission distances are measured and given in Fig. 11. It can be observed that output power is relatively stable when the transmission distance changes from $20mm$ to $70mm$, which is one of the advantages of LCL compensation over SS compensation, and maximum power can be transferred when the distance is $50mm$. When the transmission distance becomes larger, the efficiency reduced because of the decreasing of coupling coefficient. The highest efficiency, which is 65%, can be obtained when transmitting power over $20mm$. The load is another factor with a significant influence on output power and efficiency. When transmitting power over $20mm$, the output power and efficiency with different loads are measured and given in Fig. 12. Maximum power can be transferred when the load is 40Ω, and the efficiency increases as load resistance increases. Finally, the steady-state voltage and current waveform of both transmitter and receiver are measured and shown in Fig. 13, in which the load is 70 Ω, the transmission distance is $20mm$, and the operating frequency is $120kHz$. It is clear that the voltage and current of the receiver have no phase difference. In order to achieve ZVS, the inverter operates in the inductive region and the transmitter current lags the voltage. Detailed parameters of the proposed system are given in Table. II

V. Conclusion

The physical capacitor used in the compensation network of the RWPT system inevitably increases size and cost, and reduces reliability. In this paper, a novel self-compensated planar coil is proposed for the RWPT system,utilizing intra-winding capacitance to form a resonant tank. The physical capacitor can therefore be eliminated and the proposed RWPT system can achieve self-compensation. Higher intra-winding capacitance can be obtained by connecting multi-layer PCB coils in parallel, which significantly reduces the resonant frequency of the proposed RWPT system. LCL compensation is used to reduce the power fluctuation when the transmission distance changes, and reduce spikes during switching transitions within the inverter. The theoretical basis of the proposed RWPT system was comprehensively studied. Simulation was conducted to initially investigate the performance of the system. The same transmitter and receiver were designed by connecting six four-layer PCBs in parallel. Experimental measurements were conducted to further explore the performance. The results show that intra-winding capacitance can be effectively used for compensation and no additional physical capacitors are needed.

TABLE II: Parameters of the system

Item	Value
Input voltage	$100V$
Output voltage	$68.5V$
Coil inductance	$129uH$
Parasitic capacitance	$20nF$
Coil size	$23 \times 22 \times 9.6cm^3$
Output power	$67W$
Efficiency	65%
MOSFET	$IRFP4868PBF$
Diode	$VS-60APH03-N3$

References

[1] M. Mohammad, E. T. Wodajo, S. Choi, and M. E. Elbuluk, "Modeling and design of passive shield to limit EMF emission and to minimize shield loss in unipolar wireless charging system for EV," IEEE Trans. Power Electron., vol. 34, no. 12, pp. 12235–12245, Dec. 2019.

[2] S. Y. Hui, "Planar wireless charging technology for portable electronic products and Qi," Proc. IEEE, vol. 101, no. 6, pp. 1290–1301, Jun. 2013.

[3] X. Li, C.-Y. Tsui, and W.-H. Ki, "A 13.56 MHz wireless power transfer system with reconfigurable resonant regulating rectifier and wireless power control for implantable medical devices," IEEE J. Solid-State Circuits, vol. 50, no. 4, pp. 978–989, Apr. 2015.

[4] Z. Yan, Y. Zhang, T. Kan, F. Lu, K. Zhang, B. Song, and C. Mi, "Frequency Optimization of a Loosely Coupled Underwater Wireless Power Transfer System Considering Eddy Current Loss," IEEE Trans. Ind. Electron., vol. 66, no. 5, pp. 3468–3476, May. 2019.

[5] S. Y. R. Hui and W. C. Ho, "A new generation of universal contactless battery charging platform for portable consumer electronic equipment," IEEE Trans. Power Electron., vol. 20, no. 3, pp. 620–627, May 2005.

[6] A. Kurs, A. Karalis, R. Moffatt, J. D. Joannopoulos, P. Fisher, and M. Solja˘ci´c, "Wireless power transfer via strongly coupled magnetic resonances," Science, vol. 317, no. 5834, pp. 84–86, Jul. 2007.

[7] M. Budhia, G. A. Covic, and J. T. Boys, "Design and optimization of circular magnetic structures for lumped inductive power transfer systems," IEEE Trans. Power Electron., vol. 26, no. 11, pp. 3096–3108, Nov. 2011.

[8] M. Budhia, J. T. Boys, G. A. Covic, and C.-Y. Huang, "Development of a single-sided flux magnetic coupler for electric vehicle IPT charging systems," IEEE Trans. Ind. Electron., vol. 60, no. 1, pp. 318–328, Jan. 2013.

[9] G. Nagendra, G. Covic, and J. Boys, "Determining the physical size of inductive couplers for IPT EV systems," IEEE J. Emerg. Sel. Topics Power Electron., vol. 2, no. 3, pp. 571–583, Sep. 2014.

[10] Y. Li, T. Lin, R. Mai, L. Huang, and Z. He, "Compact double-sided decoupled coils based WPT systems for high power applications: Analysis, design and experimental verification," IEEE Trans. Transp. Electrific., vol. 4, no. 1, pp. 64–75, Mar. 2018

[11] W. X. Zhong, C. Zhang, X. Liu, and S. Y. R. Hui, "A methodology for making a three-coil wireless power transfer system more energy efficient than a two-coil counterpart for extended transfer distance," IEEE Trans. Power Electron., vol. 30, no. 2, pp. 933–942, Feb. 2015.

[12] J. Zhang, X. Yuan, C. Wang, and Y. He, "Comparative analysis of two-coil and three-coil structures for wireless power transfer," IEEE Trans. Power Electron., vol. 32, no. 1, pp. 341–352, Jan. 2017.

[13] Z. H. Ye, Y. Sun, X. Dai, C. S. Tang, Z. H. Wang, and Y. G. Su, "Energy efficiency analysis of U-coil wireless power transfer system," IEEE Trans. Power Electron., vol. 31, no. 7, pp. 4809–4817, Jul. 2016.

[14] S. Moon, B. C. Kim, S. Y. Cho, C. H. Ahn, and G. W. Moon, "Analysis and design of a wireless power transfer system with an intermediate coil for high efficiency," IEEE Trans. Ind. Electron., vol. 61, no. 11, pp. 5861–5870, Nov. 2014.

[15] S. Cheon, Y.-H. Kim, S.-Y. Kang, M. L. Lee, J.-M. Lee, and T. Zyung, "Circuit-model-based analysis of a wireless energy-transfer system via coupled magnetic resonances," IEEETrans. Ind. Electron., vol. 58, no. 7, pp. 2906–2914, Jul. 2011.

[16] D. H. Tran, V. B. Vu, and W. J. Choi, "Design of a high efficiency wireless power transfer system with intermediate coils for the on-board chargers of electric vehicles," IEEE Trans. Power Electron., vol. 33, no. 1, pp. 175–187, Jan. 2018.

[17] Y. Zhang, Z. Zhao, and T. Lu, "Quantitative analysis of system efficiency and output power of four-coil resonant wireless power transfer," IEEE J. Emerg. Sel. Topics Power Electron., vol. 3, no. 1, pp. 184–190, Mar. 2015.

[18] J. P. W. Chow, N. Chen, H. S. H. Chung, and L. L. H. Chan, "An investigation into the use of orthogonal winding in loosely coupled link for improving power transfer efficiency under coil misalignment," IEEE Trans. Power Electron., vol. 30, no. 10, pp. 5632–5649, Nov. 2014.

[19] W. M. Ng, C. Zhang, D. Lin, and S. Y. R. Hui, "Two- and three-dimensional omnidirectional wireless power transfer," IEEE Trans. Power Electron., vol. 29, no. 9, pp. 4470–4474, Sep. 2014.

[20] W. Zhang, S.-C. Wong, C. K. Tse, and Q. Chen, "Analysis and comparison of secondary series- and parallel-compensated inductive power transfer systems operating for optimal efficiency and load-independent voltage-transfer ratio," IEEE Trans. Power Electron., vol. 29, no. 6, pp. 2979–2990, Jun. 2014.

[21] N. Bailian, C. Y. Chung, and H. L. Chan, "Design and comparison of parallel and series resonant topology in wireless power transfer," in Proc. IEEE 8th Conf. Ind. Electron. Appl., Melbourne, Australia, 2013, pp. 1832–1837.

[22] E. R. Joy, B. K. Kushwaha, G. Rituraj, and P. Kumar, "Analysis and comparison of four compensation topologies of contactless power transfer system," in Electric Power and Energy Conversion Systems (EPECS), 2015 4th International Conference on, Nov 2015, pp. 1–6.

[23] C. Jiang, K. T. Chau, C. Liu, and C. H. Lee, "An overview of resonant circuits for wireless power transfer," Energies, vol. 10, no. 7, p. 894, Jun. 2017.

[24] N. A. Keeling, G. A. Covic, and J. T. Boys, "A unity-power-factor IPT pickup for high-power applications," IEEE Trans. Ind. Electron., vol. 57, no. 2, pp. 744–751, Feb. 2010.

[25] A. A. S. Mohamed, A. Berzoy, F. G. N. de Almeida, and O. Mohammed, "Modeling and assessment analysis of various compensation topologies in bidirectional IWPT system for EV applications," IEEE Trans. Ind. Appl., vol. 53, no. 5, pp. 4973–4984, Sep. 2017.

[26] C.-S. Wang, G. A. Covic, and O. H. Stielau, "Investigating an LCL load resonant inverter for inductive power transfer applications," IEEE Trans. Power Electron., vol. 19, no. 4, pp. 995–1002, Jul. 2004.

[27] F. Lu, H. Zhang, H. Hofmann, W. Liu, and C. Mi, "An inductive and capacitive integrated coupler and its LCL compensation circuit design for wireless power transfer," in Proc. IEEE Energy Convers. Congr. Expo., 2016, pp. 1–5.

[28] J. Li and D. Costinett, "Analysis and design of a series self-resonant coil for wireless power transfer," in Proc. IEEE Appl. Power Electron. Conf. Expo., San Antonio, TX, USA, 2018, pp. 1052–1059.

[29] M. A. Saket, M. Ordonez, and N. Shafiei, "Planar transformers with near-zero common-mode noise for flyback and forward converters," IEEE Trans. Power Electron., vol. 33, no. 2, pp. 1554–1571, Feb. 2018.